Inorganic Chemistry

Article

Dynamic Axial Ligand-Site Exchange in Facially Discriminated Ruthenium(II) Carbonyl and Rhodium(III) Halide Metalloporphyrins

Maxwell J. Gunter* and Kathleen M. Mullen

Chemistry, School of Biological and Biomedical Sciences, University of New England, Armidale, NSW 2351, Australia

For a series of six-coordinate Ru^{II}(CO)L or Rh^{III}(X$^-$)L porphyrins, which are facially differentiated by having a naphthoquinol- or hydroquinol-containing strap across one face, we show that ligand migration from one face to the other can occur under mild conditions and that ligand-site preference is dependent on the nature of L and X$^-$. For bulky nitrogen-based ligands, the strap can be displaced sideways to accommodate the ligand on the same side as the strap. For the ligand pyrazine, we show ^{1}H NMR evidence for monodentate and bridging binding modes on both faces, dependent on ligand concentration and metalloporphyrin structure, and that interfacial migration is rapid under normal conditions. For monodentate substituted pyridine ligands, there is a site-dependence on structure, and we show clear evidence of dynamic ligand migration through a series of ligand-exchange reactions.

Introduction

The use of porphyrins as constituents is a pervasive theme in the design and construction of supramolecular systems of ever-increasing sophistication and complexity.[1] Metalloporphyrins have been incorporated as addressable components in a variety of assemblies, particularly catenanes and rotaxanes,[2-7] and their rich coordination chemistry has been invoked frequently in templating[8] and self-assembly[9] roles for the ordered construction of complex systems. Most commonly, zinc is used as the central metal ion, as it has the desirable attributes that suit its function in these roles: it is easily inserted into and removed from porphyrins, it is diamagnetic, it has well-studied photophysical characteristics,[3,10] and it forms relatively stable five-coordinate complexes with nitrogen-donor atom ligands. On the other hand, the moderate stability (K_a's typically of 10^2 to 10^4) and lability of the complexes result in ligand-exchange processes that are typically fast on the ^{1}H NMR chemical-shift time scale, so that the spectra are often complicated by exhibiting single (and often broadened) time-averaged, temperature-dependent signals for both bound and unbound forms. This factor can also be a hindrance in using zinc metalloporphyrins in templating roles for omplex systems, unless there are significant cooperative effects in multicomponent assemblies. In such systems, the increased stability and inertness of systems deliberately designed for maximal fit and complementarity of ligand guest or adjuvants has been used to good effect both in templating during assembly and in functional roles of the final supramolecule.[11,12]

* To whom correspondence should be addressed. E-mail: mgunter@une.edu.au. Tel.: +612 6773 2767. Fax: +612 6773 3268.

(1) Raymo, F. M.; Stoddart, J. F. In *Supramolecular Organization and Materials Design*; Jones, W., Rao, C. N. R., Eds.; Cambridge University Press: Cambridge, U.K., 2002; pp 332–362. Balzani, V.; Credi, A.; Venturi, M. *Proc. Natl. Acad. Sci. U.S.A.* **2002**, *99*, 4814–4817. Balzani, V.; Credi, A.; Venturi, M. *Chem.—Eur. J.* **2002**, *8*, 5525–5532. Stoddart, J. F. *Acc. Chem. Res.* **2001**, *34*, 410–411.

(2) Linke, M.; Fujita, N.; Chambron, J. C.; Heitz, V.; Sauvage, J. P. *New J. Chem.* **2001**, *25*, 790–796. Ogoshi, H.; Mizutani, T.; Hayashi, T.; Kuroda, Y. In *The Porphyrin Handbook*; Kadish, K. M., Smith, K. M., Guilard, R., Eds.; Academic Press: San Diego, CA, 2000; Vol. 6, pp 279–341. Chambron, J.-C.; Heitz, V.; Sauvage, J.-P. In *The Porphyrin Handbook*; Kadish, K. M., Smith, K. M., Guilard, R., Eds.; Academic Press: San Diego, CA, 2000; Vol. 6, pp 1–41. Chou, J.-H.; Kosal, M. E.; Nalwa, H. S.; Rakow, N. A.; Suslick, K. S. In *The Porphyrin Handbook*; Kadish, K. M., Smith, K. M., Guilard, R., Eds.; Academic Press: San Diego, CA, 2000; Vol. 6, pp 43–131. Maitra, U.; Balasubramaniam, R. In *Supramolecular Organization and Materials Design.*; Jones, W., Rao, C. N. R., Eds.; Cambridge University Press: Cambridge, U.K., 2002; pp 363–390. Solladie, N.; Chambron, J. C.; Sauvage, J. P. *J. Am. Chem. Soc.* **1999**, *121*, 3684–3692. Chichak, K.; Walsh, M. C.; Branda, N. R. *J. Chem. Soc., Chem. Commun* **2000**, 847–848. Andersson, M.; Linke, M.; Chambron, J. C.; Davidsson, J.; Heitz, V.; Sauvage, J. P.; Hammarstrom, L. *J. Am. Chem. Soc.* **2000**, *122*, 3526–3527. Andersson, M.; Linke, M.; Chambron, J.-C.; Davidsson, J.; Heitz, V.; Hammarstrom, L.; Sauvage, J.-P. *J. Am. Chem. Soc.* **2002**, *124*, 4347–4362. Coumans, R. G. E.; Elemans, J.; Thordarson, P.; Nolte, R. J. M.; Rowan, A. E. *Angew. Chem., Int. Ed.* **2003**, *42*, 650–654. Ballester, P.; Costa, A.; Deya, P. M.; Frontera, A.; Gomila, R. M.; Oliva, A. I.; Sanders, J. K. M.; Hunter, C. A. *J. Org. Chem.* **2005**, *70*, 6616–6622.

For those systems where complex stability and ligand specificity are important factors, ruthenium(II) and rhodium-(III) have been utilized in place of zinc.[13,14] Ruthenium(II) carbonyl complexes of porphyrins have a high affinity for nitrogen-based ligands, with K_a's on the order of 10^6 to 10^9. The fast ligand-on rates and slow ligand-off rates lead to slow exchange on the NMR chemical-shift time scale, so that separate resonances are observed for bound and unbound species. Likewise, Rh^{III} halide complexes have even higher stability constants and similar NMR behavior. In each case, the metals are six-coordinate, the fifth ligand being CO for Ru^{II} and X^- for Rh^{III}, and any added nitrogen base L forms stable species [RuP(CO)L] or [RhP(X)L]. Because of the high binding constants, equimolar mixtures of nitrogen base and these metalloporphyrins show essentially quantitatively bound complexes in the NMR spectra, uncomplicated by all but the smallest traces of free ligand.

The exact nature of the ruthenium and rhodium derivatives that are generally used as starting materials in these studies is often undefined; depending on the metal insertion process and subsequent workup procedures, the sixth coordination site on the metal ion is often assumed to be variously methanol, water, solvent, or metal–metal association in a dimeric species.[13,15] In any event, the overwhelming affinity for both metalloporphyrin derivatives for nitrogen- or phosphorus-based ligands ensures the rapid and complete replacement of the sixth ligand to produce the RuP(CO)L or RhP(X)L species.[16] Under normal conditions, the carbonyl ligand in the rutheniu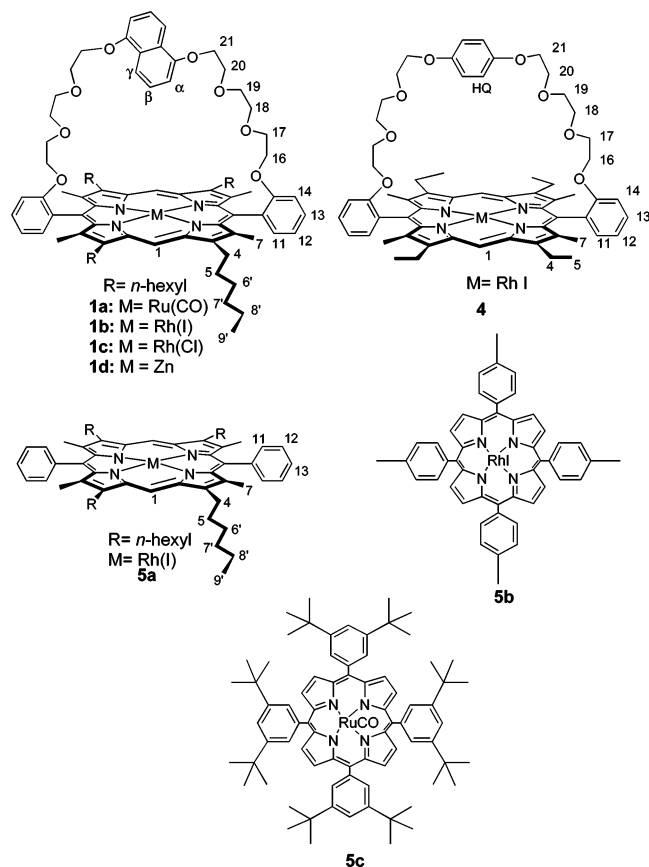m and the halide ion in the rhodium derivatives remain intact and are considered to be nonlabile. Indeed, it has been claimed that the carbonyl in the RuP-(CO)L species (where L is a nitrogen-donor ligand) can only be replaced by an exogenous ligand to form the RuPL₂ species under midwavelength irradiation (such as that provided by a mercury vapor lamp). An exception to this is when L is a phosphorus-donor atom ligand, when the CO is displaced under dark conditions to form the six-coordinate bisphosphino or mixed nitrogen/phosphino complexes.[17] Likewise, the RhP(X)L species do not readily form the bis-[RhPL₂]X species even in the presence of a vast excess of L, except for the phosphorus-based ligands, which readily form the symmetrical diaxially coordinated species.[18]

Indeed, these particular properties have been used to advantage in several recent examples of supramolecular systems.[6,16,18−20] In most instances where these metalloporphyrin derivatives have been utilized, ligand-binding-site discrimination has not been an issue, as facially symmetrical porphyrins have generally been used. Even for those systems where the final assembly can result in spatially differentiated sites, free rotation about bonds connecting the porphyrin components ensures that the most-stable thermodynamic species result, without recourse to facial ligand-site exchange at the metal ion in the porphyrin.[12,16,20,21] In a specific example of a triangular-cyclic Ru^{II}(CO) porphyrin trimer, templating by a tripyridyltriazine ligand leads to efficient assembly of the trimer with the template occupying the inside of the cavity; without the template, a mixture of dimers, trimers, and tetramers, with the coordinated CO ligands occupying both the interior and exterior positions of the cavity, is obtained.[22]

On the other hand, we have used a variety of facially encumbered ("functionalized picket-fence"-type) and strapped porphyrins for the assembly of a wide range of catenanes, pseudo-rotaxanes, and rotaxanes.[4,7,23] For a series of strapped porphyrins, we have produced multiporphyrin supramolecular systems using both thermodynamic (metal-ion coordination) and kinetic (covalently attached) principles in both solution

(3) Flamigni, L.; Heitz, V.; Sauvage, J.-P. *Struct. Bonding (Berlin, Ger.)* **2006**, *121*, 217−261. Flamigni, L.; Talarico, A. M.; Chambron, J. C.; Heitz, V.; Linke, M.; Fujita, N.; Sauvage, J. P. *Chem.—Eur. J.* **2004**, *10*, 2689−2699.

(4) Gunter, M. J. *Eur. J. Org. Chem.* **2004**, 1655−1673. Gunter, M. J.; Farquhar, S. M.; Mullen, K. M. *New J. Chem.* **2004**, *28*, 1443−1449.

(5) Gunter, M. J.; Bampos, N.; Johnstone, K. D.; Sanders, J. K. M. *New J. Chem.* **2001**, *25*, 166−173.

(6) Ikeda, T.; Asakawa, M.; Shimizu, T. *New J. Chem.* **2004**, *28*, 870−873.

(7) Gunter, M. J.; Merican, Z. *Supramol. Chem.* **2005**, *00*, 1−9.

(8) Sanders, J. K. M. *Pure Appl. Chem.* **2000**, *72*, 2265−2274.

(9) Bouamaied, I.; Coskun, T.; Stulz, E. *Struct. Bonding (Berlin, Ger.)* **2006**, *121*, 1−47. Kobuke, Y. *Struct. Bonding (Berlin, Ger.)* **2006**, *121*, 49−104. Iengo, E.; Scandola, F.; Alessio, E. *Struct. Bonding (Berlin, Ger.)* **2006**, *121*, 105−143. Hupp, J. T. *Struct. Bonding (Berlin, Ger.)* **2006**, *121*, 145−165. Burrell, A. K.; Officer, D. L.; Plieger, P. G.; Reid, D. C. W. *Chem. Rev.* **2001**, *101*, 2751−2796. Imamura, T.; Fukushima, K. *Coord. Chem. Rev.* **2000**, *198*, 133−156.

(10) Flamigni, L.; Talarico, A. M.; Serroni, S.; Puntoriero, F.; Gunter, M. J.; Johnston, M. R.; Jeynes, T. P. *Chem.—Eur. J.* **2003**, *9*, 2649−2659.

(11) Sanders, J. K. M. *Chem.—Eur. J.* **1998**, *4*, 1378−1383. Nakash, M.; Clyde-Watson, Z.; Feeder, N.; Davies, J. E.; Teat, S. J.; Sanders, J. K. M. *J. Am. Chem. Soc.* **2000**, *122*, 5286−5293.

(12) Mak, C. C.; Bampos, N.; Sanders, J. K. M. *Chem. Commun.* **1999**, *21*, 1085−1086. Webb, S. J.; Sanders, J. K. M. *Inorg. Chem.* **2000**, *39*, 5912−5919.

(13) Sanders, J. K. M.; Bampos, N.; Clyde-Watson, Z.; Darling, S. L.; Hawley, J. C.; Kim, H.-J.; Mak, C. C.; Webb, S. J. In *The Porphyrin Handbook*; Kadish, K. M., Smith, K. M., Guilard, R., Eds.; Academic Press: New York, 2000; Vol. 3, Chap. 15, p 1.

(14) Sanders, J. K. M. In *The Porphyrin Handook*; Kadish, K. M., Smith, K. M., Guilard, R., Eds.; Academic Press: New York, 2000; Vol. 3, Chap. 22, p 347.

(15) Collman, J. P.; Hutchison, J. E.; Lopez, M. A.; Guilard, R. *J. Am. Chem. Soc.* **1992**, *114*, 8066−8073.

(16) Stulz, E.; Scott, S. M.; Ng, Y. F.; Bond, A. D.; Teat, S. J.; Darling, S. L.; Feeder, N.; Sanders, J. K. M. *Inorg. Chem.* **2003**, *42*, 6564−6574.

(17) Stulz, E.; Maue, M.; Feeder, N.; Teat, S. J.; Ng, Y. F.; Bond, A. D.; Darling, S. L.; Sanders, J. K. M. *Inorg. Chem.* **2002**, *41*, 5255−5268. Stulz, E.; Sanders, J. K. M.; Montalti, M.; Prodi, L.; Zaccheroni, N.; De Biani, F. F.; Grigiotti, E.; Zanello, P. *Inorg. Chem.* **2002**, *41*, 5269−5275.

(18) Stulz, E.; Maue, M.; Scott, S. M.; Mann, B. E.; Sanders, J. K. M. *New J. Chem.* **2004**, *28*, 1066−1072.

(19) Zheng, J. Y.; Tashiro, K.; Hirabayashi, Y.; Kinbara, K.; Saigo, K.; Aida, T.; Sakamoto, S.; Yamaguchi, K. *Angew. Chem. Int. Ed.* **2001**, *40*, 1858−1861. Fukushima, K.; Funatsu, Y.; Ichimura, A.; Sasaki, Y.; Suzuki, M.; Fujihara, T.; Tsuge, K.; Imamura, T. *Inorg. Chem.* **2003**, *42*, 3187−3193. Stulz, E.; Scott, S. M.; Bond, A. D.; Otto, S.; Sanders, J. K. M. *Inorg. Chem.* **2003**, *42*, 3086−3096. Kim, H. J.; Redman, J. E.; Nakash, M.; Feeder, N.; Teat, S. J.; Sanders, J. K. M. *Inorg. Chem.* **1999**, *38*, 5178−5183. Ikeda, T.; Asakawa, M.; Goto, M.; Nagawa, Y.; Shimizu, T. *Eur. J. Org. Chem.* **2003**, 3744−3751. Redman, J. E.; Feeder, N.; Teat, S. J.; Sanders, J. K. M. *Inorg. Chem.* **2001**, *40*, 3217−3221.

(20) Redman, J. E.; Feeder, N.; Teat, S. J.; Sanders, J. K. M. *Inorg. Chem.* **2001**, *40*, 2486−2499.

(21) Kim, H. J.; Bampos, N.; Sanders, J. K. M. *J. Am. Chem. Soc.* **1999**, *121*, 8120−8121. Mak, C. C.; Bampos, N.; Darling, S. I.; Montalti, M.; Prodi, L.; Sanders, J. K. M. *J. Org. Chem.* **2001**, *66*, 4476−4486.

(22) Marvaud, V.; Vidal-Ferran, A.; Webb, S. J.; Sanders, J. K. M. *J. Chem. Soc., Dalton Trans.* **1997**, 985−990.

studies[5,7,24] and tethered to solid supports.[25] For the reversibly assembled systems, ruthenium and rhodium porphyrins have been key components, taking full advantage of the desirable properties mentioned above. In these cases, using ruthenium and rhodium stoppers for rotaxane synthesis, for example, facial ligand-site discrimination has not been an issue, as facially symmetrical porphyrins have been used.[26]

R= *n*-hexyl
1a: M= Ru(CO)
1b: M = Rh(I)
1c: M = Rh(Cl)
1d: M = Zn

M= Rh I
4

R= *n*-hexyl
M= Rh(I)
5a

5b

5c

Figure 1. Schematic illustrating templated catenane formation utilizing strong pyridine/metalloporphyrin coordination and a neutral naphthodiimide unit. The pyridine unit must be bound preferentially underneath the strap for effective templating. Protonation of the pyridine, addition of exogenous competing ligand L′, or removal of the metal ion are several of many factors that can be used to reversibly drive the catenane, causing rotation of the entrapped macrocycle. Similar concepts relying on the templating ability of an appropriately functionalized pyridine can be used to assemble multistation rotaxanes with a variety of "innocent" or "active" (e.g., porphyrin) stopper groups.

rotaxanes, which can be addressed or "driven" by several different stimuli or inputs.[27]

These ideas are cartooned in Figure 1, using a catenane as an example. Similar concepts can lead to multistation rotaxanes of varying complexity. The naphthoquinol or hydroquinol porphyrins to be utilized in this design principle are those of the types **1** and **4**.

Experimental Section

Full experimental details for the preparation of the strapped porphyrins and their Ru[II]CO and Rh[III]X derivatives and the ligands **2** and **8** are described in the Supporting Information.

All ^{1}H NMR spectra were acquired in CDCl₃ on a Bruker AC-300P FT spectrometer at 303 K, unless otherwise stated. Chemical shifts are reported in ppm relative to the residual solvent. Deuterated chloroform was stored over molecular sieves and used without further purification.

Results and Discussion

A key requirement in such a design is that the templating pyridine-based ligand is preferentially bound "underneath" or "inside" the strap and thus that the carbonyl (in the case of the ruthenium derivative) or the halide (for the rhodium analogue) should occupy the outside coordination site.

Furthermore, it should be noted that for these strapped porphyrin derivatives, the inside and outside faces are structurally defined, and the two sites cannot easily be exchanged by degenerative atropisomeric rotation around the *meso*-phenyl to porphyrin bonds; this is hindered by the adjacent methyl and hexyl substituents at the β-pyrrolic positions. Nevertheless, for analogous functionalized porphyrins with longer tetraethylene glycol straps on either side of the naphthoquinol unit (compared with the triethylene glycol straps of the porphyrins studied here) and with less bulky ethyl rather than hexyl side chains, in some instances we have isolated "twisted" or cis and trans isomers during their synthesis. We have shown that these will atropisomerize

However, we have become interested in using ruthenium and rhodium derivatives of our strapped porphyrins as effective templates for a new range of catenanes and rotaxanes. In this design, we intend to use the templating effect resulting from the strong coordination of an appropriately substituted pyridine-based component to produce nonsymmetrical dual-functionalized catenanes or multistation
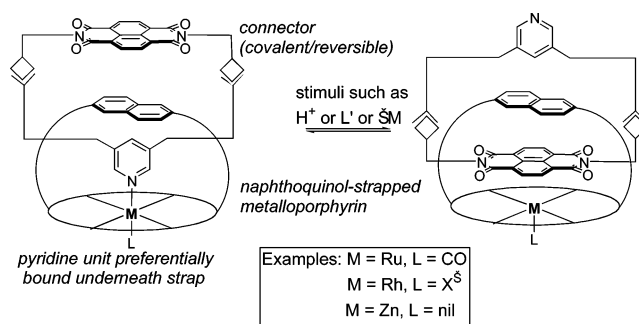
(23) Gunter, M. J.; Johnston, M. R. *J. Chem. Soc., Perkin Trans.* **1994**, *1*, 995−1008. Gunter, M. J.; Hockless, D. C. R.; Johnston, M. R.; Skelton, B. W.; White, A. H. *J. Am. Chem. Soc.* **1994**, *116*, 4810−4823. Gunter, M. J.; Farquhar, S. M.; Jeynes, T. P. *Org. Biomol. Chem.* **2003**, *1*, 4097−4112. Gunter, M. J.; Farquhar, S. M. *Org. Biomol. Chem.* **2003**, *1*, 3450−3457. Gunter, M. J.; Jeynes, T. P.; Turner, P. *Eur. J. Org. Chem.* **2004**, 193−208.

(24) Johnstone, K. D.; Yamaguchi, K.; Gunter, M. J. *Org. Biomol. Chem.* **2005**, *3*, 3008−3017. Kieran, A. L.; Pascu, S. I.; Jarrosson, T.; Gunter, M. J.; Sanders, J. K. M. *Chem. Commun.* **2005**, 1842−1844.

(25) Johnstone, K. D.; Bampos, N.; Sanders, J. K. M.; Gunter, M. J. *New J. Chem.* **2006**, *30*, 861−867. Johnstone, K. D.; Bampos, N.; Sanders, J. K. M.; Gunter, M. J. *Chem. Commun.* **2003**, 1396−1397.

(26) A distinction needs to be made between inherent facial discrimination in a structurally asymmetric porphyrin such as **1** or **4** and the inevitable facial discrimination that results from two different axial ligands at the metal center. For example, a MP(X)L complex will have facial distinction, although the free-base porphyrin need not, as is the case for peripherally substituted flat porphyrin derivatives such as **5**.

(27) The weaker binding and lability of zinc porphyrins renders them less suitable in this design motif.

to equilibrium mixtures of cis and trans isomers only slowly (e.g., 30 days at room temperature or 3 h in refluxing acetonitrile).[23e] For the shorter strap derivatives used in this work, we have not encountered any evidence of trans isomers, and after more than 24 h of refluxing in toluene or other solvents, there is no evidence of any changes that might indicate equilibration via atropisomerization. Conversely, low-temperature NMR spectra show no evidence of any slowed equilibration processes. This therefore renders unlikely a process of rapid inside−outside site exchange involving atropisomeric "flipping" of the strap in these systems, especially within timescales of seconds to minutes at ambient temperature, and assures the structural integrity of the strapped porphyrins.[28]

For 3,5-disubstituted pyridines with polar substituents (such as esters or amides), we anticipated inside stabilization by dipolar and charge-transfer interactions between the substituents and the hydroquinol or naphthoquinol groups, as well as the ethyleneoxy components of the connecting strap itself. Nevertheless, this needed to be tested, in fact, and would thus depend on the configuration of the starting solvated (methanol in our case) derivative. With the assumption that the carbonyl or halide ligands were nonlabile, the required configurations were those with the methanol inside designated RuP(CO)$_{out}$(MeOH)$_{in}$ or RhP(X)$_{out}$(MeOH)$_{in}$. Potential H bonding of the coordinated methanol with the oxygens on the strap was considered to be a significant factor influencing an inside site preference.

Even in the absence of a suitable crystal structure, the solution conformation needed to be established. This was not obvious from the results of the usual spectroscopic techniques. The sharpness of the NMR spectra in all cases, over a range of temperatures, indicated a single isomeric form of the porphyrin rather than an equilibrating mixture. The coordinated methanol could easily be identified in the ^{1}H NMR spectrum, strongly shielded, as expected. However, its position was variable, and it was clear that it was in fast exchange on the NMR chemical-shift time scale, dependent on the concentration of methanol or moisture in the solvent. The ^{13}C chemical shift of the carbonyl ligand in the ruthenium case was not diagnostic and appeared at about the same field as that for typical structurally similar but symmetrical porphyrin analogues. The proton resonance of the components in the strap were clearly affected, but it was not obvious to what extent this was due to nearby ligands or to the overall electronic effects of the ligand field associated with the coordinated metal ion. Alternative less-direct strategies were required.

Defining the Configuration−Bulky Ligand Coordination. For example, with the assumption of no carbonyl ligand exchange, it was anticipated that a bulky nitrogen-based ligand such as **2** might allow distinction between the outside and inside coordination environments for the carbon mon-
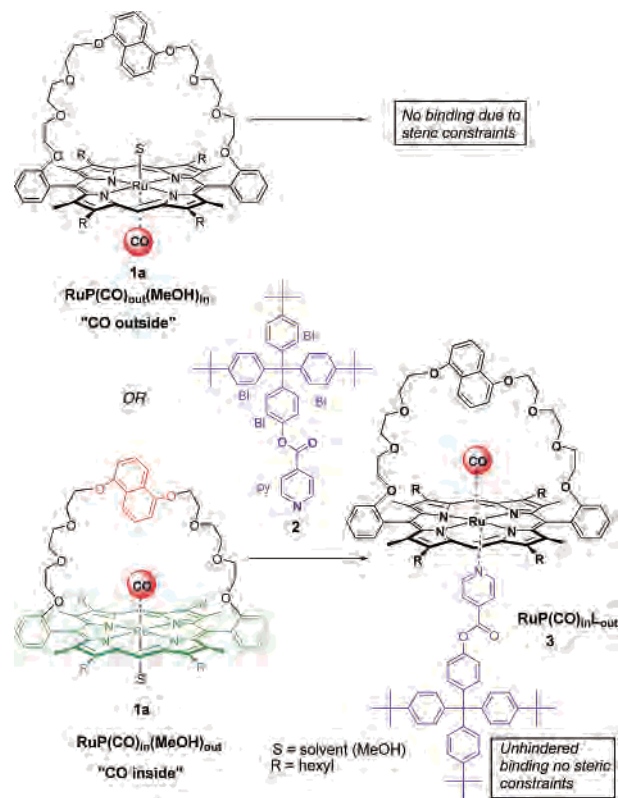

Figure 2. Schematic showing the two possible outcomes of bulky pyridine ligand **2** binding to a ruthenium naphthoquinol-strapped porphyrin with the coordinated CO in inside or outside positions. The lettering and color coding correspond to the NMR spectral assignments in Figure 3.

oxide; if it were bound outside, then coordination to the trans position by a sterically demanding ligand would be hindered by the naphthoquinol strap (Figure 2). This would be manifested in a low or zero ligand-association constant, compared with the alternative case, where access to the unhindered face of the porphyrin would result in binding constants in the normal range for nitrogen-based ligands on typical unencumbered ruthenium carbonyl porphyrins.

Thus, the ^{1}H NMR spectra of mixed solutions of ruthenium porphyrin **1a** and bulky pyridine **2** (which was shown by simple models to be too bulky to fit under the strap of the porphyrin in its most-extended conformation) showed all species in slow exchange on the NMR chemical-shift time scale. Nonstoichiometric mixtures showed peaks due to both bound and unbound species, and the chemical shifts of both species did not vary with changes in stoichiometry. The pyridine resonances shifted from the unbound positions of 8.87 and 8.01 ppm to the bound positions of 5.58 and 1.32 ppm, respectively. At 1:1 stoichiometry, the pyridine was essentially fully bound, as expected for the typically strong binding of pyridine-based ligands to Ru(CO) porphyrins (K_a typically 10^6−10^8 M^{-1}).

At first sight, the strong binding might have indicated coordination to the open face. Nevertheless, the spectrum (Figure 3, part B) showed obvious asymmetry of the porphyrin resonances, showing two sets of peaks for the meso protons (1, light green), and the hexyl and methyl side chains (4, 5, 7, 6′−9′, dark green), and the OCH$_2$ protons (16) were diastereotopically split. On the other hand, only one set of

---

(28) Sanders and Redman (Redman, J. E.; Sanders, J. K. M. *Org. Letters* **2000**, *2*, 4141−4144) have also reported atropisomerization in strapped porphyrins systems, which have chain lengths comparable to those of tetraethylene glycol straps, but with a disulfide linkage rather than a bulky naphthoquinol unit in the center; nevertheless, these too show slow equilibration of the cis and trans forms (1 h in refluxing toluene).
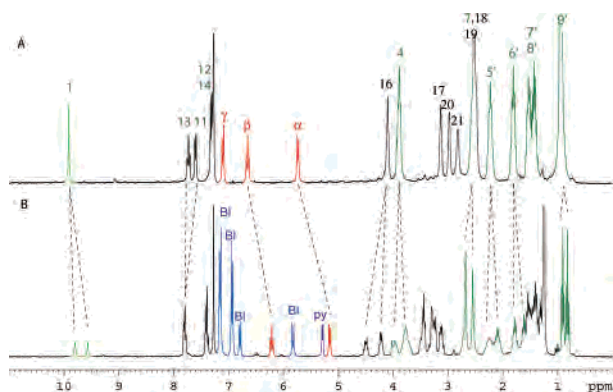
Figure 3. NMR comparison of the ruthenium-strapped porphyrin **1a** (A) and the 1:1 mixture of ruthenium porphyrin **1** with pyridine ligand **2** (B). Colors and labeling refer to structure **1a** and Figure 2. Spectra are assigned by COSY and NOESY and ROESY techniques (see Supporting Information, Figures S1−S3).

peaks was observed for the naphthalene aromatic protons (α, β, γ, red) in the strap and the pyridine ligand resonances (py, purple). The spectrum was neither time- nor temperature-dependent, indicating a single, nonequilibrating species in solution.

Similar asymmetry was observed for the corresponding rhodium iodo complexes of both the naphthoquinol **1b** and hydroquinol **4** derivatives, indicating that the asymmetry was not metal-ion specific and that effects due to the aromatic group of the strap were not the cause of the splitting. Furthermore, the fact that the rhodium iodo derivative of the unstrapped analogue **5a** produced symmetrical spectra under the same conditions (see Supporting Information, Figure S4) precluded effects due to the restricted rotation of the bulky ligand or any interference from the hexyl side chains.

The unsymmetrical NMR spectra can be accounted for by the bulky pyridine binding on the *same* side of the porphyrin as the strap, with the strap displaced to one side of the porphyrin to accommodate the bulky ligand. This structure **6** is further supported by the fact that the bound-pyridine resonances in **2** are more upfield in the strapped porphyrins than in the corresponding unstrapped ruthenium **5c** and rhodium **5a** and **5b** porphyrins, as a result of shielding by the contiguous aromatic groups in the strap. There are also clear NOE and ROESY correlations between the pyridine protons and nearby ethoxy protons in the strap (particularly protons 18−20) of both porphyrin **1** and **4**, consistent with configurations as depicted for **6** (see Supporting Information, Figure S3). Single resonances for the aromatic groups of the strap and the pyridine ligand and its substituent indicate unrestricted rotational freedom in these regions of the molecules at these temperatures.[29]

This then appeared to confirm that both the CO and I⁻ ligands are in the outside positions in both the Ru and Rh porphyrin derivatives **1a** and **1b** and **4**. It was thus presumed that the ligated methanol in all of the metalloporphyrins as
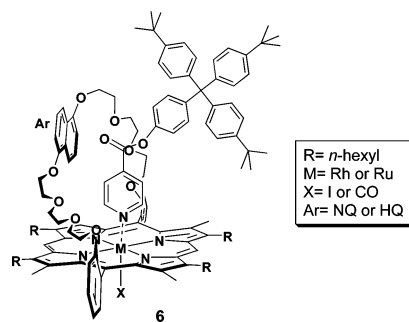
isolated must occupy an inside position, and it is this ligand that is displaced by added nitrogenous ligands. In each case, it was thus concluded that the formulation would be $RuP(CO)_{out}L_{in}$ or $RhPI_{out}L_{in}$ for the respective species as isolated from the thermodynamically controlled metalation processes.

Although having established that the bulky pyridine **2** occupies the inside coordination site, and despite efforts to restrict its binding to the outside position, we wished to seek confirmatory evidence to establish the scope and generality of this behavior. Furthermore, the conclusions were based on the assumption that there is no exchange of the CO or I⁻ ligands under these conditions. Such a generality demanded more definitive proof.

Defining the Configuration−Bridging Ligand Coordination. As an alternative approach to defining the preferred binding site of pyridine-based ligands, the coordination behavior of a bridging ligand such as pyrazine was studied. It was rationalized that if the pyrazine bound in a similar fashion to the pyridine ligand **2** (inside), only a monomeric 1:1 species, $MP(X)_{out}pz_{in}$ (Type II, Figure 4), would be formed. Despite the evidence above demonstrating the flexibility of the strap, it was deemed that a dimeric [MP-$(X)_{out}]_2pz_{in}$ species (Type I, Figure 4), in which the strap on each porphyrin is displaced to one side to accommodate the other, would be too sterically hindered in this case with such a short bridging ligand.

An analogous NMR titration was thus performed with ruthenium porphyrin **1a** and pyrazine (Figure 5). At up to 0.5 equiv of pyrazine per mole of porphyrin, the spectrum showed evidence of three species, including starting porphyrin (Figure 5, blue).[30] Only two sets of pyrazine protons could be identified, a singlet at −0.93 ppm (Figure 5, red), and an AX pattern at 5.78 and 1.40 ppm (Figure 5, green). The singlet was typical of a symmetrical complex with the pyrazine binding in bridging mode. This component was also characterized by a single meso peak at 9.34 ppm (Figure 5, part B), which precluded it from being the dimeric [RuP-$(CO)_{out}]_2pz_{in}$ species (Type I, Figure 4). Its spectrum is only consistent with a 2:1 [RuP(CO)_{in}]_2pz_{out} formulation with the CO ligand constrained to the inside coordination site (Type III, Figure 4). The second coordinated species (Figure 5, green) was identified as a 1:1 complex having pyrazine

(29) It is not immediately apparent why the more-stable binding site for this bulky ligand is in the inside position, but $\pi-\pi$ interactions between the aromatic groups of the ligand and the naphthoquinol or hydroquinol units may be a contributing factor.

(30) To assist the reader in interpreting the expected relationship between the symmetry, splitting pattern, chemical shift, and integration expected for each of the Type I−V structures, Table S1 is included in the Supporting Information.
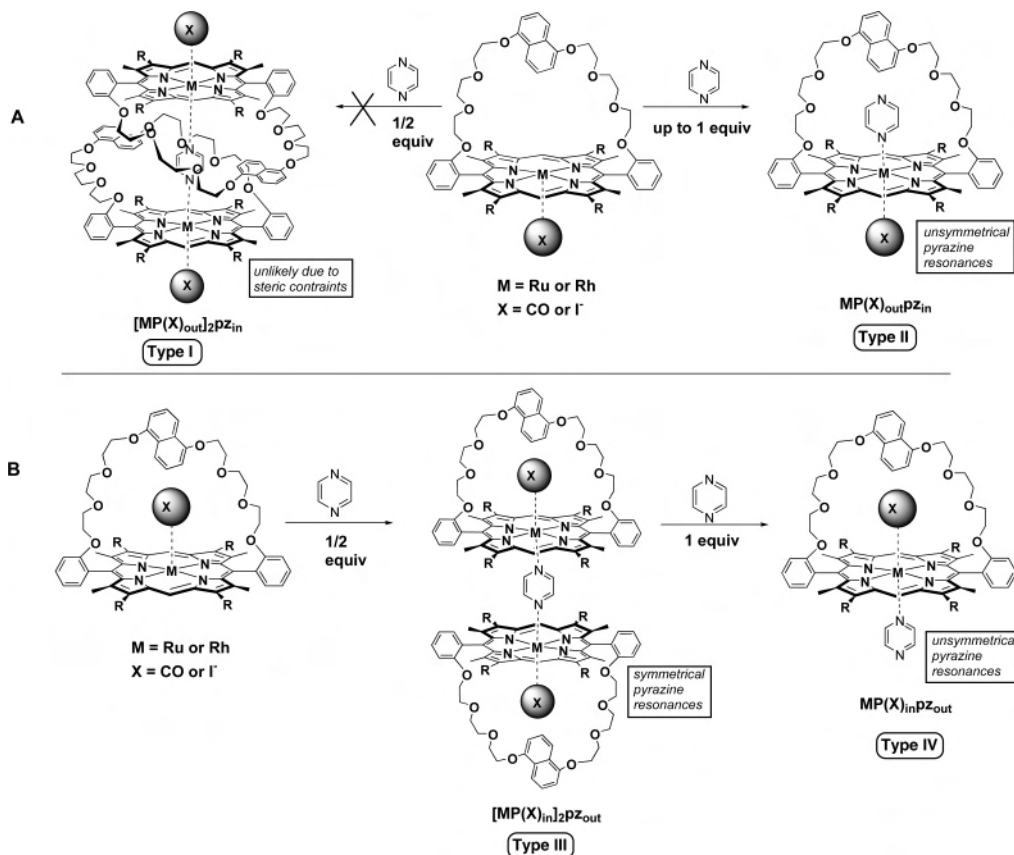
Figure 4. (A) Possible species produced by titration of Ru/Rh porphyrins and pyrazine for the CO/I⁻ ligand occupying the outside coordination site. (B) Possible species produced by the titration of Ru/Rh porphyrins and pyrazine for the CO/I⁻ ligand occupying the inside coordination site.
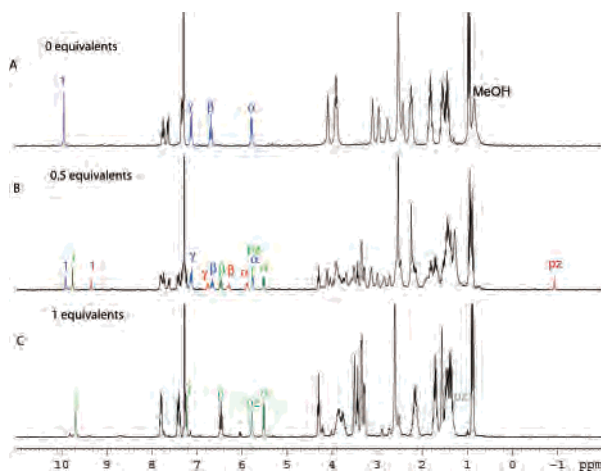

Figure 5. NMR titration of Ru porphyrin **1a** with an increasing number of pyrazine equivalents. Blue peaks and numbers indicate starting porphyrin material, red indicates a dimeric [RuP(CO)$_{in}$]$_2$pz$_{out}$ species, and green indicates a monomeric RuP(CO)$_{out}$pz$_{in}$ species throughout. The spectral assignments are discussed in the text. Spectral integrations are displayed in the Supporting Information, Figure S5.

bound in a monodentate mode, with one meso resonance at 9.76 ppm and a characteristic unsymmetrical AX splitting pattern for the pyrazine protons (5.78 and 1.40 ppm).[31] Because the pyridine proton resonances are further upfield in this species than its unstrapped porphyrin counterparts **5c**, this monomeric species was assigned as one in which the pyrazine occupies the inside binding site, (RuP(CO)$_{out}$pz$_{in}$) (Type II, Figure 4).

The addition of >0.5 equiv of pyrazine resulted in the gradual disappearance with increasing pyrazine concentration of the dimeric complex ([RuP(CO)$_{in}$]$_2$pz$_{out}$, red, Figure 5) (Type III, Figure 4) until at 1:1 equiv only the monomeric (RuP(CO)$_{out}$pz$_{in}$, green, Figure 5) (Type II, Figure 4) complex remained. Confirmation of the assignment of this species as Type II was provided by a clear NOE correlation between the pyrazine β-proton signal with that of the ethyleneoxy protons at position 20 in the strap (see Supporting Information, Figures S6 and S7)).

This implies that for the ruthenium carbonyl porphyrin derivatives **1a**, the CO ligand is capable of exchanging binding sites from inside to outside during the course of the titration. Hence, the binding of added pyridine-like ligands to either side of the strapped porphyrins is possible, and the final site preference will be dictated by thermodynamic and kinetic principles.

Analogous studies were carried out on the rhodium iodide derivatives **1b** of the same strapped porphyrin, to ascertain the propensity for site exchange of the iodide ion. In an NMR titration, the pyrazine was shown to effectively bind to the rhodium porphyrin in slow exchange on the NMR chemical-

(31) Unlike typical facially symmetrical and unencumbered ruthenium porphyrins such as **5c**, throughout the entire titration (even as low as 0.15 equiv of added ligand), both monodentate and bridging pyrazine-bound species were present. This relative destabilization of the bridging-mode species in favor of the monodentate may be due to the additional steric hindrance created by the hexyl side chains in the strapped derivatives compared with that of the flat porphyrins, as seen in previously reported studies.[20]
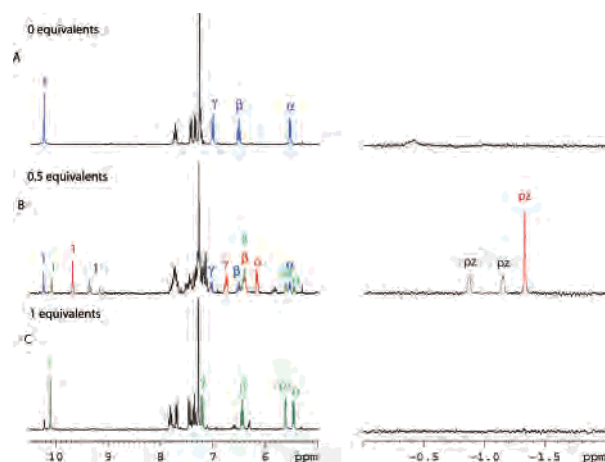
Figure 6. Titration of rhodium iodide porphyrin **1b** with an increasing number of pyrazine equivalents. Blue indicates the starting porphyrin, red indicates the dimeric $[RhP(I)_{in}]_2pz_{out}$ species, brown indicates a proposed $RhP(I)_{out}pz_{in/out}(I)_{in}PRh$ species, and green indicates the $RhP(I)_{out}pz_{in}$ species. The assignments are discussed in the text.

Figure 7. Proposed structure for the $RhP(I)_{out}pz_{in/out}(I)_{in}PRh$ species formed during the titration of **1** with pyrazine, described in Figure 6 (brown).

shift time scale; however, when 0.5 equiv of pyrazine was added, the resulting spectra indicated the presence of additional species compared with those obtained for the corresponding ruthenium porphyrin (Figure 6).

At 0.5 equiv of added pyrazine, *six* peaks were observed for the *meso*-porphyrin protons (1) in the NMR spectrum. Three of these can easily be accounted for, being the proton at 10.24 ppm (Figure 6, blue) corresponding to starting porphyrin material; the proton at 10.10 ppm (Figure 6, green) resulting from the $RhP(I)_{out}pz_{in}$ species (Type II, Figure 4),[32] with corresponding pyrazine protons at 5.61 and 0.89 ppm; and the proton at 9.69 ppm (Figure 6, red) corresponding to the symmetrical $[RhP(I)_{in}]_2pz_{out}$ sandwich like complex (Type III, Figure 4) with its associated pyrazine singlet at -1.32 ppm. These species were analogous to those seen in the titrations of both the ruthenium and rhodium "flat" or facially symmetrical porphyrins such as **5b**[33] and **5c**[22] and also the unsymmetrical **1a**, with pyrazine.[34] The remaining three peaks of the porphyrin meso protons (Figure 6, brown) were associated with a species having a corresponding pyrazine doublet at -0.87 and -1.15 ppm. Such upfield chemical shifts for *both* pyrazine sets of protons are indicative of bridging pyrazine coordination; however, the AB pattern indicates an unsymmetrical structure, implying a different coordination environment at each end of the pyrazine ligand.

(32) As in the case for ruthenium porphyrin **1a**, the pyrazine protons of this species are shifted further upfield than for the unstrapped porphyrin **5b**. Thus, the resulting 1:1 species is assigned as one in which the pyrazine occupies the inside binding site, $RhP(I)_{out}pz_{in}$. NOE and ROESY correlations between the pyrazine and nearby ethoxy protons in the strap of the porphyrin support such a structure.

(33) Wayland, B. B.; van Voorhees, S. L.; Wilker, C. *Inorg. Chem.* **1986**, *25*, 4039−4042.

(34) The 1:1 and 2:1 species were assigned based on their characteristic NMR patterns: the 1:1 species has a single peak for the *meso*-porphyrin protons and a corresponding pyrazine doublet with an AX splitting pattern; the 2:1 species likewise has a single *meso*-porphyrin peak but with a single pyrazine peak (see Supporting Information, Table S1). However, unlike the flat or unencumbered porphyrins, the appearance of the 1:1 species at this low concentration of pyrazine suggests that the formation of the dimeric 2:1 species is less favored for these more sterically substituted porphyrin derivatives, as discussed previously.[29]
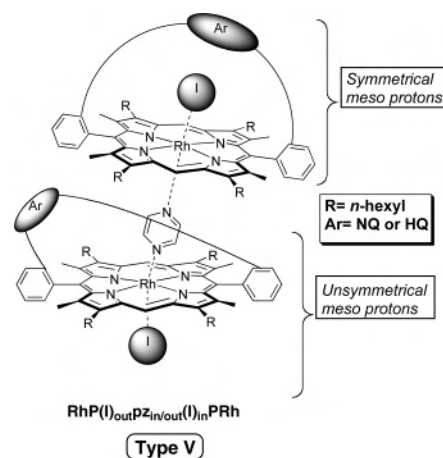
This, together with the fact that the meso protons are three-way inequivalent, indicates a second unsymmetrical 2:1 species. This is consistent with a conformation in which the strap is displaced over one-half of a porphyrin (as seen for the bulky pyridine ligands discussed above) and coordinating to one end of the pyrazine, with the other pyrazine N bound to the outside position of a second porphyrin; this species is thus designated $RhP(I)_{out}pz_{in/out}(I)_{in}PRh$ (Type V, Figure 7).

At more than 0.5 equiv of pyrazine, both the 2:1 species, $RhP(I)_{out}pz_{in/out}(I)_{in}PRh$ (Type V) and $[RhP(I)_{in}]_2pz_{out}$ (Type III) were replaced, on increasing pyrazine concentration, by the single 1:1 species $RhP(I)_{out}pz_{in}$ (Type II, Figure 4) with corresponding pyrazine protons at 5.61 and 0.89 ppm (Figure 6, green).

This study thus clearly shows that pyrazine can bind to both the inside and outside coordination sites, and so the I^- ligand must be capable of exchange between each face of the porphyrin, contrary to previous assumptions.

Further evidence of this site-exchange process was also found in an analogous titration with the *hydroquinol*-strapped rhodium porphyrin **4** and pyrazine (Figure 8). However, in this case at up to 0.5 equiv of added pyrazine, only *five* resonances were observed for the *meso*-porphyrin protons, one of which was attributed to the starting porphyrin (10.19 ppm) and a second (9.70 ppm) to the symmetrical $[RhP(I)_{in}]_2pz_{out}$ 2:1 species (Type III, Figure 4) with its corresponding pyrazine singlet at -1.42 ppm. Three of the remaining smaller meso-proton resonances were assigned to the unsymmetrical 2:1 $RhP(I)_{out}pz_{in/out}(I)_{in}PRh$ species (Type V) with its corresponding pyrazine doublets at -0.98 and -1.22 ppm. The lack of a 1:1 $RhP(I)_{out}pz_{in}$ (Type II, Figure 4) species at this stage in the titration (as compared with the hexyl-substituted naphthoquinol porphyrin derivative) indicates that in this case there is no preferential formation of the dimeric 1:1 species in favor of a 2:1 complex and, hence, no 1:1 species is formed until more than 0.5 equiv of pyrazine is added. This is presumably due to the less sterically demanding ethyl side chains compared with the hexyl chains in porphyrins **1a** and **1b**.[20]

The addition of more than 0.5 equiv of pyrazine again resulted in the gradual decay of the 2:1 species with
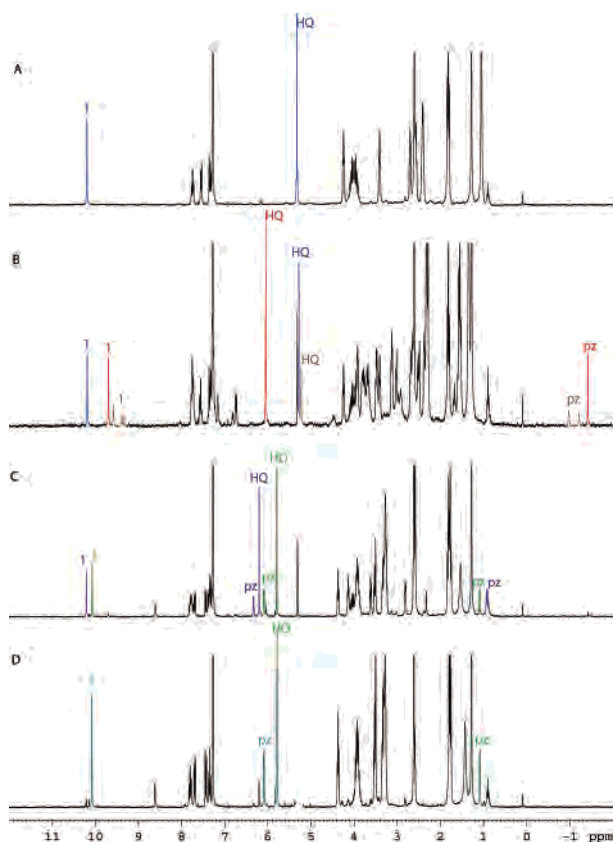
Figure 8. Titration of rhodium porphyrin **4** with pyrazine. Spectrum A shows the starting porphyrin (blue); spectrum B is with 0.4 equiv of added pyrazine (brown, indicating the proposed RhP(I)$_{out}$pz$_{in/out}$(I)$_{in}$PRh species), and red indicates the [RhP(I)$_{in}$]$_2$pz$_{out}$ species. Spectrum C is the spectrum obtained when 1 equiv of pyrazine is added, taken immediately after the final addition (purple indicates RhP(I)$_{in}$pz$_{out}$ and green indicates RhP-(I)$_{out}$pz$_{in}$), and spectrum D indicates a 1:1 mixture of porphyrin and pyrazine after equilibration over 24 h.

increasing pyrazine concentration; however, in this case, initially, *two* distinct 1:1 species were present in solution (Figure 8C), as evidenced by two sets of peaks for both porphyrin and pyrazine resonances. One of these 1:1 species had a meso-proton resonance at 10.21 ppm with corresponding pyrazine peaks at 6.33 and 0.93 ppm and a hydroquinol proton peak at 6.20 ppm (Figure 8, purple). These peaks are attributed to the 1:1 RhP(I)$_{in}$pz$_{out}$ species (Type IV, Figure 4) with the pyrazine binding to the outside face and were a result of the gradual dissociation of the 2:1 [RhP(I)$_{in}$]$_2$pz$_{out}$ species (Type III, Figure 4) with increasing pyrazine concentration. The other 1:1 species had a meso-proton resonance at 10.08 ppm, pyrazine peaks at 6.08 and 1.09 ppm, and a hydroquinol proton peak at 5.79 ppm (Figure 8, green); this is consistent with a RhP(I)$_{out}$pz$_{in}$ species (Type II, Figure 4).[35] However, over time (several hours at ambient temperature), this spectrum resolved into that of the single, more-stable monomeric RhP(I)$_{out}$pz$_{in}$ species (Type II) at the expense of the RhP(I)$_{in}$pz$_{out}$ 1:1 species (Type IV) (Figure 8D).

---

(35) The α protons in the coordinated pyrazine are affected overwhelmingly by the porphyrin shielding in both "pz-in" and "pz-out" cases, and, hence, the shifts are not very different in either case. The β protons are more affected by the naphthoquinol in the pz-in case and, in fact, are deshielded to some extent, as a result of possible edge-to-face aromatic interactions under the naphthoquinol ring.

This observation is especially significant as it is the first clear and unequivocal evidence for I$^-$ ligand exchange in Rh^{III} porphyrins. Although the mechanism for the exchange process is unknown, this experiment also shows that the exchange process is slower for the hydroquinol-strapped Rh porphyrin **4** than for the naphthoquinol analogue **1b**, as the exchange of the two 1:1 species into a single more-stable isomer was clearly more rapid for **1b** and was not observed on a similar time scale at room temperature for this system. The reason for this is still unknown; however, it is clear that small differences in structure can result in large changes in the kinetics of this process, a fact that may prove useful in the design of supramolecular interlocked systems.

Coordination Site Preference–Ligand Dependence. Clearly, the lability and site exchange of the carbon monoxide and iodide ion in these ruthenium and rhodium porphyrins has significant implications for the use of strapped porphyrins for templated rotaxane and catenane syntheses. Thus, the site preferences for several different pyridine ligands were compared: pyridine itself, dimethyl pyridine-3,5-dicarboxylate (**7**) and the corresponding triethyleneglycol ester (**8**), the latter two representing substituted pyridine-based ligands that might be used in templated catenane or rotaxane synthesis.

The ^{1}H NMR spectra of the 1:1 ruthenium porphyrin **1a**/pyridine mixtures indicated virtually complete complexation of the ligands and a slow exchange environment. The resonances for the *meso*-porphyrin protons shifted typically upfield after addition of all three pyridine ligands. For pyridine, the naphthoquinol α proton was shielded; however, for pyridines **7** and **8**, this proton was deshielded (Supporting Information, Figure S8). Whereas the protons in pyridine **7** and **8** have identical chemical shifts to those bound to an unstrapped porphyrin control **5c**, the unsubstituted pyridine protons are more upfield-shifted, indicating a shielding by the aromatic protons in the strap of the porphyrin. This strongly suggests that pyridine occupies the inside coordination site RuP(CO)$_{out}$(py)$_{in}$, whereas the ligands **7** and **8** occupy the outside position RuP(CO)$_{in}$(Rpy)$_{out}$ (Figure 9).

Furthermore, 2D NOESY and ROESY NMR experiments revealed that for the pyridine complex, there were some correlations with nearby ethoxy protons in the strap of the porphyrin; the complexes with the ligands **7** and **8** showed no such correlations. This confirms that the binding of pyridine ligands **7** and **8** to ruthenium-strapped porphyrin **1a** is to the open face, a conformation clearly unsuitable for the proposed design for catenane and rotaxane synthesis.

For the corresponding rhodium porphyrin derivative **1b**, in an equimolar mixture with either of the pyridine ligands **7** and **8**, the chemical shift of the 4′-pyridine proton at 7.15 ppm in each case was identical to that for the same ligand with a facially symmetrical porphyrin **5b** (Supporting Information, Figure S9). This and the fact that no NOE or ROESY correlations could be detected with any protons of the strap or of the naphthoquinol implies an outside coordination site for these ligands, RhP(I)$_{in}$(Rpy)$_{out}$ (Figure 9). Despite this, significant shifts in the ethoxy protons (16–21) and the naphthoquinol protons (α, β, γ) in the strap over
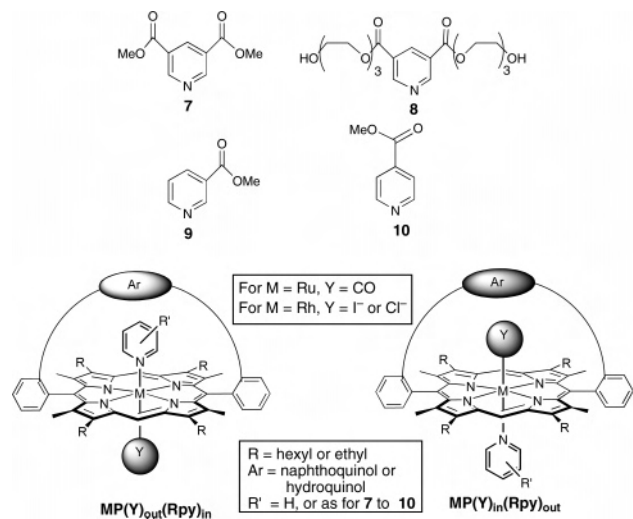
Figure 9. Substituted pyridines used in the ligand-dependence study of the strapped porphyrins and the possible site preferences for pyridine and ligands **7**−**10**, as discussed in the text.
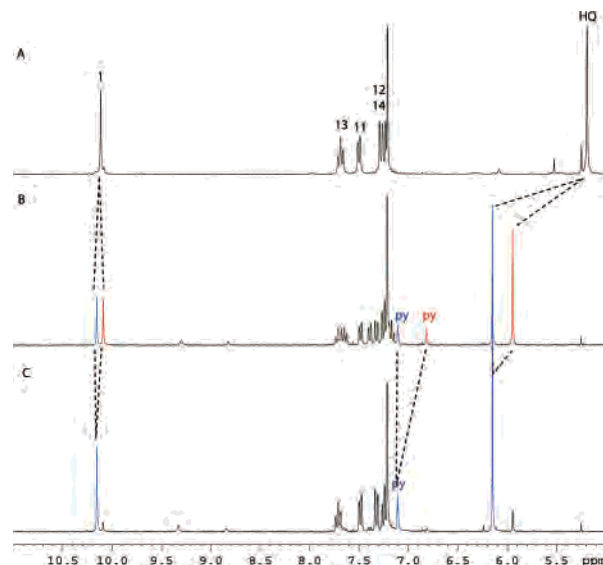

Figure 10. Binding of pyridine ligand **7** to hydroquinol rhodium porphyrin **4**. Spectrum A is that of the Rh porphyrin **4**. Spectrum B is a 1:1 mixture of **4** and **7** immediately after ligand addition. Spectrum C is that of **4** and **7** after 24 h.

the porphyrin were evident and can be explained by the iodide ion exchanging from the outside site in the starting methanol complex to the inside coordination site. For pyridine itself, on the other hand, an upfield shift of the pyridine resonances in a 1:1 mixture and relevant NOE and ROESY correlations indicated an inside binding preference for this unsubstituted pyridine ligand, RhP(I)$_{out}$(py)$_{in}$ (Figure 9). Likewise, the monoester pyridine derivatives **9** and **10** also exhibited an inside site preference, RhP(I)$_{out}$(Rpy)$_{in}$ (Figure 9 and Supporting Information, Figure S10). It was also noted that the α proton of the naphthoquinol is a useful indicator of inside vs outside coordination: for those ligands that bind at an inside position (**9**, **10**, and pyridine itself), the α proton has an upfield, shielded shift relative to that of the starting material, whereas for the pyridines that bind outside (ligands **7** and **8**), a deshielded or downfield shift is observed.

Clearly, for these systems, there is a subtle thermodynamic balance for the site preference of both the iodide and pyridine ligands, and both contribute to the overall free energy of the final complex. Thus, the corresponding *hydroquinol*-strapped porphyrin **4** with less π dispersal than the naphthoquinol counterpart would be expected to influence both the iodide ion or pyridine ligand to a greater or lesser extent. Accordingly, an equimolar solution of rhodium hydroquinol porphyrin and the pyridine diester ligand **7** showed evidence of *both* inside (Figure 10, red) and outside (Figure 10, blue) coordination within minutes of mixing, but over about 24 h at room temperature, the spectrum slowly decayed to that of a single outside coordinated pyridine isomer (Figure 10).

The inside-coordinated methanol of the starting porphyrin complex **4** is rapidly exchanged initially on addition of pyridine **7** to give the kinetic product RhP(I⁻)$_{out}$(Rpy)$_{in}$ (Figure 10, red). In a slower process, the thermodynamic product RhP(I⁻)$_{in}$(Rpy)$_{out}$ (Figure 10, blue) is then formed (Figures 9 and 10). For the corresponding naphthoquinol derivative **1b**, although the final outcome is the analogous RhP(I⁻)$_{in}$(Rpy)$_{out}$ isomer, no evidence was seen for the

initially formed converse isomer.[36] This may be due to either a faster exchange process in this case or, alternatively, that the iodide ligand is already in the inside position in the initial complex, stabilized by a more effective p−π interaction with the larger π cloud of the naphthalene unit compared with the smaller phenyl of the hydroquinol-strapped derivative. Nevertheless, it is clear that the ligand-site preference in these systems is finely balanced, and this may be used to advantage in the design strategy.[37]

For example, an alternative to reducing the π density of the aromatic unit in the strap to destabilize iodide interactions is to maintain the naphthoquinol unit but to exchange the iodide for a harder chloride ligand, as in **1c**. This strategy is successful, and in a corresponding NMR experiment in this instance, the initially produced kinetic product RhP(Cl)$_{out}$-(Rpy)$_{in}$ only slowly converts to the more-stable RhP(Cl)$_{in}$-(Rpy)$_{out}$ over several days at room temperature in CDCl$_3$ solution (Figure 9 and Supporting Information, Figure S11). This can now allow sufficient time for any subsequent templating reaction for this strategy to be used in supramolecular assembly processes, providing that conditions of low temperature and reasonably fast reactions can be chosen.

Coordination Site Preference−Ligand Exchange. Indeed, simple exchange experiments involving combinations of ligands can be utilized to confirm the general principles

---

(36) The limited range of ligand combinations tested in this study militates against a definitive rationalization of the factors involved in ligand-site preference. However, one such factor may involve electronic repulsions between the ligands and the naphthoquinol or hydroquinol units of the strap. Computed electron densities for the ligands **7**, **9**, **10**, and pyridine indicate increased electron density in the region adjacent to the electron-rich units of the straps for **7** compared with those of **9**,**10**, and pyridine, and this would indicate a destabilization of **7** relative to the other ligands. Calculated electrostatic potential diagrams are given in the Supporting Information, Figure S15.

(37) Although we have not encountered any examples where the final outcome is an equilibrating mixture in these limiting systems, we predict that for other combinations of ligands, an equilibrium mixture of both isomers might well be present under ambient conditions.
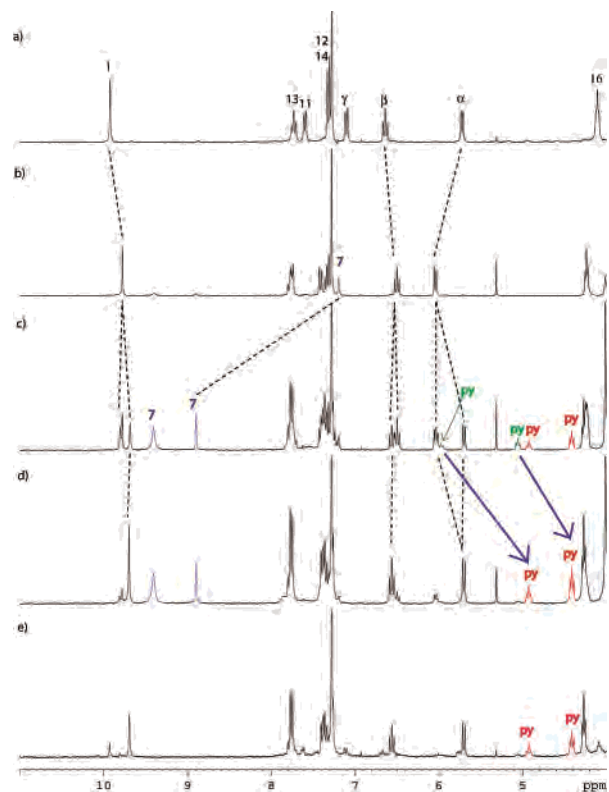
Figure 11. NMR spectrum obtained during competition experiments between the binding of pyridine itself and ligand **7** with Ru porphyrin **1a**. Spectrum a is that of of **1a**; spectrum b is that of an equimolar mixture of **1a** and **7**; spectrum c is that of spectrum b after the addition of 1 equiv of pyridine; spectrum d is that of spectrum c after 30 min. The blue peaks indicate protons associated with pyridine **7**. The green peaks indicate pyridine bound on the outside position of porphyrin **1a**, and the red peaks indicate pyridine bound inside the cavity of **1a**.

of site preference and ligand exchange. For example, as established above, an equilibrated equimolar mixture of strapped ruthenium porphyrin **1a** and diester pyridine **7** contains exclusively the RuP(CO)$_{in}$(Rpy)$_{out}$ species.

On the addition of 1 mol equiv of unsubstituted pyridine, it immediately binds to the outside position in a step that presumably involves the simple substitution of the weaker pyridine ligand **7**; the difference in ligand strength ensures virtually complete substitution, and resonances of the free ligand **7** are now evident (Figure 11). This is followed by slower exchange over about 30 min of the pyridine to the inside binding site and the concomitant exchange of the CO ligand to the outside (Figure 12). Spectrum c in Figure 11 clearly shows both pyridine-bound isomers, RuP(CO)$_{in}$(py)$_{out}$ (green) and RuP(CO)$_{out}$(py)$_{in}$ (red)[38] (see also Figure 12). Significantly, the final spectrum is identical to that obtained when pyridine is added directly to ruthenium porphyrin **1a** in the absence of substituted pyridine **7** (Figure 11e). This is unequivocal evidence for CO site migration, that the process is conservative and no aspect of the system is

(38) The relative assignment of these two species was based on the premise that the more-downfield pair of pyridine 4- and 3,5-protons (5.91 and 5.03 ppm, respectively, green, Figure 11) appeared in about the same position as those for pyridine binding to a reference flat porphyrin **5c** and, hence, are indicative of the RuP(CO)$_{in}$(py)$_{out}$ isomer; the more upfield pair (4.87 and 4.42 ppm, red, Figure 11), shielded by the aromatic group in the strap, belong to the RuP(CO)$_{out}$(py)$_{in}$ species.
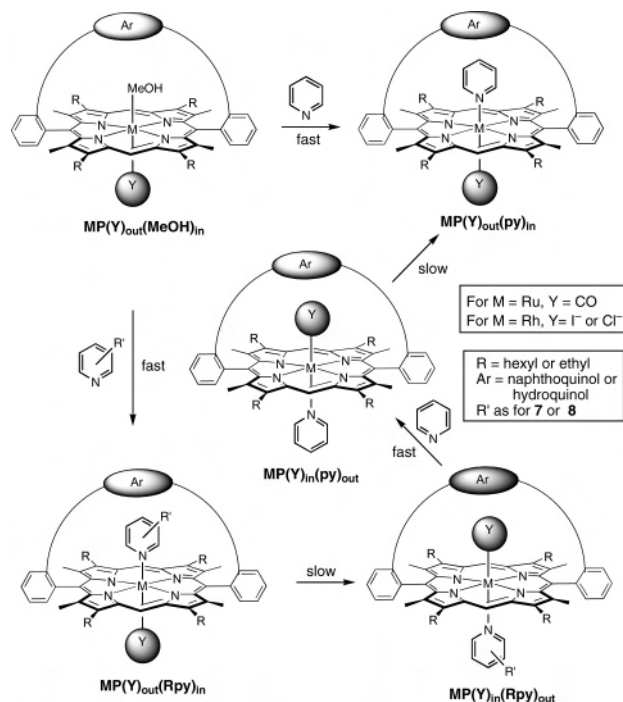

Figure 12. Representation of the ligand-site preferences and ligand-exchange processes for Ru- and Rh-strapped porphyrin derivatives.

compromised, and, especially, that there is no loss of gaseous CO in the exchange process.

In an analogous experiment using the hydroquinol rhodium porphyrin **4**, similar results were obtained (Supporting Information, Figure S12); however, the time taken to re-establish equilibrium after pyridine addition was noticeably longer (2 days compared with 30 min). Similar to the ruthenium system, the initially formed rhodium isomer RhP(I$^-$)$_{in}$(py)$_{out}$ slowly converted to the RhP(I$^-$)$_{out}$(py)$_{in}$ isomer (Figure 12), as indicated by the slow disappearance of the downfield pair of pyridine resonances (5.90 and 4.95 ppm) at the expense of the growth of the more-shielded upfield pair (4.76 and 4.31 ppm). NOE correlations between the pyridine 3′ protons and methylenes of the strap confirmed the inside configuration (see Supporting Information, Figures S13 and S14). Again, it is apparent that not only do the pyridine and I$^-$ ligands exchange coordination sites but that this occurs via a conservative mechanism, as evidenced by the fact that the resulting spectrum is identical to that obtained when pyridine is added directly to rhodium porphyrin **1b** (Supporting Information, Figure S12E).

Mechanistic Implications. Although we have not attempted a detailed mechanistic or kinetic study of the ligand-site-exchange processes described here, we can offer several observations that may have implications for a ligand-exchange mechanism. We are not aware of any detailed studies of the mechanism of ligand exchange in ruthenium-(II) carbonyl and rhodium(III) halide porphyrins. However, Merbach et al.[39] concluded in a study of ligand exchange in a hexacoordinate ruthenium(II) carbonyl complex that a dissociative mechanism was not in operation because no

(39) Aebischer, N.; Churland, L. D.; Dolci, L.; Frey, U.; Merbach, A. E. *Inorg. Chem.* **1998**, *37*, 5915−5924.

diffusional loss of CO was observed; for a series of square-planar rhodium(I) complexes studied by Garrou and Hartwell,[40] it was established that exchange of CO occurred through an associative process involving a carbonyl-bridging five-coordinate intermediate. In our systems, the conservative nature of the ligand-exchange reactions indicates no diffusional loss of gaseous CO. We have also established that the ligand-exchange processes are not light-dependent and are not effected by added CO or excess halide ligands. Any process involving atropisomerization allowing facial exchange of the hydroquinol or naphthoquinol straps by a rotation or twisting process can also be ruled out, as discussed above, by the fact that in some instances the ligand-exchange reactions are complete within seconds to minutes at ambient temperature.

Nevertheless, ligand-site exchange is clearly demonstrated in these systems, regardless of a defined mechanism.

Conclusion

We interpret the results provided by these experiments as clear and unambiguous evidence for carbonyl and halide ligand-site exchange in $Ru^{II}CO$ and $Rh^{III}X$ metalloporphyrins. For facially equivalent porphyrins, such processes are product degenerative and are thus generally undetected and, indeed, in many cases inconsequential.

However, for facially unsymmetrical porphyrin systems, including assemblies where porphyrin facial discrimination arises as a result of overall symmetry and geometry constraints (for example, in multiporphyrin "tweezers", cyclic arrays, or other nonlinear systems), then ligand geometry at the axial positions of the metalloporphyrin can lead to geometric or regioisomerism. This can have critical consequences for any subsequent manipulations involving ligand exchange, especially if one of the axial sites is nonlabile. For metalloporphyrins involving organometallic σ or π bonding, such as in ruthenium(II) or rhodium(III) porphyrins of the type MP(R)L, where R can be CO, alkyl or aryl, or rhodium(III) halide porphyrins such as RhP(X)L, then it has previously been assumed that the axial carbon- or halide-based ligand is normally inert to exchange, except under

defined conditions such as irradiation, reduction, or exchange involving phosphorus-based ligands.

However, we have presented evidence here that for a series of strapped porphyrin derivatives, the carbonyl ligand in ruthenium(II) porphyrins and the halide in Rh^{III} porphyrins are labile, and although they are not easily exchanged by added exogenous ligands, they are susceptible to site exchange from one face of the porphyrin to the other under very mild conditions. To this extent, the geometry of the starting porphyrin should not be expected to be maintained under conditions where ligand migration is possible, and the final geometry will be dictated by thermodynamic principles.

Thus, we show that conditions of solvent, temperature, axial ligand, and added ligand can determine the most-stable coordination geometry for these types of systems. Our explanation for the results for these dynamic systems is site migration of the coordinated CO or halide ligands in the Ru^{II} and Rh^{III} derivatives in real time. The outcomes of the experiments are clear. What is not obvious, however, are the possible mechanisms by which these processes occur; this must await further definitive studies.

With the use of these principles, it is thus possible in certain instances to use both kinetic and thermodynamic control to produce either geometric isomer for a particular system. Far from being a restriction in system design involving these types of porphyrins, the thermodynamic site exchangeability can be used to advantage in templating or other assembly processes. We have illustrated this in using appropriate ligand-based templates with these types of strapped Ru^{II} and Rh^{III} porphyrins to assemble supramolecular arrays under reversible conditions. These results will be reported elsewhere.

Supporting Information Available: Experimental procedures and spectral data for all compounds; representative spectra for ^{1}H NMR titrations discussed in the text, including 2D spectra (19 pages). This material is available free of charge via the Internet at http://pubs.acs.org.

(40) Garrou, P. E.; Hartwell, G. E. *Inorg. Chem.* **1976**, *15*, 646−650.

IC062112I